Available online at www.sciencedirect.com
ScienceDirect
Bioorganic & Medicinal Chemistry 15 (2007) 1802–1807
Bioorganic & Medicinal Chemistry

Synthesis and in vivo evaluation of [^{18}F]-4-[5-(4-methylphenyl)-3-(trifluoromethyl)-1H-pyrazol-1-yl]benzenesulfonamide as a PET imaging probe for COX-2 expression

Jaya Prabhakaran,[a] Mark D. Underwood,[a,b] Ramin V. Parsey,[a,b] Victoria Arango,[a,b] Vattoly J. Majo,[a] Norman R. Simpson,[b,c] Ronald Van Heertum,[c] J. John Mann[a,b,c] and J. S. Dileep Kumar[a,b,*]

[a]*Department of Psychiatry, Columbia University College of Physicians and Surgeons, NY, USA*
[b]*Division of Neuroscience, New York State Psychiatric Institute, New York, NY 10032, USA*
[c]*Department of Radiology, Columbia University College of Physicians and Surgeons, NY, USA*

Received 2 August 2006; revised 13 November 2006; accepted 19 November 2006
Available online 29 November 2006

Abstract—Synthesis of [^{18}F]4-[5-(4-methylphenyl)-3-(trifluoromethyl)-1H-pyrazol-1-yl]benzenesulfonamide ([^{18}F]celecoxib), a selective COX-2 inhibitor, is achieved via a bromide to [^{18}F]F$^-$ exchange reaction. Synthesis of the precursor for radiolabeling was achieved from 4′-methylacetophenone in four steps with 22% overall yield. Under non-radioactive conditions, fluorination was achieved using TBAF in DMSO at 135 °C in 80% yield. Synthesis of [^{18}F]celecoxib was achieved using [^{18}F]TBAF in DMSO at 135 °C in 10 ± 2% yield (EOS) with >99% chemical and radiochemical purities. The specific activity was 120 ± 40 mCi/μmol (EOB). [^{18}F]celecoxib was found to be stable in ethanol, however, de[^{18}F]fluorination (6.5%) was observed after 4 h in 10% ethanol–saline solution. Rodent PET studies show bone labeling indicating in vivo de[^{18}F]fluorination of [^{18}F]celecoxib. PET studies in baboon indicated a lower rate of de[^{18}F]fluorination than rat and retention of radioactivity in brain regions consistent with the known distribution of COX-2. A radiolabeling method that can generate consistent high specific activity is needed for routine human use.

1. Introduction

The discovery of cyclooxygenase-2 (COX-2) and its role in inflammation led to the recognition that COX-2 selective inhibitors might have an anti-inflammatory effect without the gastrointestinal side effects of non-selective COX inhibitors.[1–6] Subsequent discoveries suggesting an involvement of COX-2 in many diseases or disease processes[7–9] raised the possibility that quantification of COX-2 expression might be a useful biological marker for early diagnosis, monitoring disease progression, and an indicator of effective treatment. Positron emission tomography (PET) is a non-invasive imaging technique used in nuclear medicine to study various biochemical and biological processes in vivo because it can detect targets at subnanomolar concentrations.[10,11] Efforts undertaken thus far to develop a specific PET probe for COX-2 expression have been unsuccessful.[12–19] Recently, synthesis and in vivo evaluation of [^{125}I]IMTP and [^{125}I]IATP are reported as potential SPECT tracers for COX-2 expression in rats.[20] The COX-2 IC_{50} values of these ligands are 5.16 and 8.20 μM and have a COX-1/COX-2 selectivity ratio of 19 and 13, respectively. The micromolar affinity and poor selectivity of [^{125}I]IMTP and [^{125}I]IATP would not qualify them as PET tracer candidates. The biodistribution studies of these ligands also show uniform retention of radioactivity in all areas examined indicating a lack of measurable specific binding. Moreover, the affinity of IMTP and IATP for other enzymes, biogenic amines, transporters, and receptors is not reported. Hence the retention of radioactivity of [^{125}I]IMTP and [^{125}I]IATP in various tissues may be due to the contribution of non-specific binding and perhaps some binding to other sites where the ligands may have higher binding affinity. Hence, currently no specific imaging agent is available for COX-2. In this report, we

Keywords: [^{18}F]Fluorine; PET; Radiotracer; Inflammation.
* Corresponding author. Tel.: +1 212 543 1163; fax: +1 212 543 1054; e-mail: dk2038@columbia.edu

0968-0896/$ - see front matter © 2006 Elsevier Ltd. All rights reserved.
doi:10.1016/j.bmc.2006.11.033

present the [^{18}F]radiolabeling of 4-[5-(4-methylphenyl)-3-(trifluoromethyl)-1H-pyrazol-1-yl]benzenesulfonamide (celecoxib), a selective COX-2 inhibitor, and the results of in vivo imaging studies in rats and baboons. COX-2 and COX-1 K_i values of celecoxib are 40 and 17,000 nM, respectively, with a COX-1/COX-2 selectivity ratio of 425.[4] These properties coupled with known safe toxicity data of celecoxib in human subjects suggest that celecoxib can be a suitable candidate PET tracer for the in vivo quantification of COX-2.

2. Results and discussion

2.1. Chemistry

Synthesis of *N*-[bis(4-methoxyphenyl)phenylmethyl]-4-[3-(bromodifluoromethyl)-5-*p*-tolylpyrazol-1-yl]benzenesulfonamide (**5**), the precursor for radiolabeling of celecoxib, and standard celecoxib was achieved as described in Scheme 1. The synthesis of 2-bromo-2,2-difluoro-1-imidazol-1-yl-ethanone (**2**) has been achieved via the N-acylation of *N*,*N*′-carbonyldiimidazole (**1**) with 2-bromo-2,2-difluoroacetyl chloride in 90% yield.[21] Reaction of 4′-methyl acetophenone with **2** afforded bromo-4,4-difluoro-1-*p*-tolylbutane-1,3-dione (**3**). The coupling reaction proceeded smoothly in 1 h to afford 65% of the dione **3** in presence of compound **2**,[22] whereas using bromodifluoroacetyl chloride as the coupling agent the reaction resulted in poor yield of **3**. A subsequent condensation reaction of **3** with 4-hydrazinobenzenesulfonamide by refluxing in ethanol resulted in the formation of 4-[3-(bromodifluoro-methyl)-5-*p*-tolyl-pyrazol-1-yl]benzenesulfonamide (**4**) in 45% yield. Compound **4** was protected as dimethoxytrityl (DMT) derivative **5**, in 82% yield.[18,19] The pharmacologic screen from NIMH-Psychoactive Drug Screening Program (PDSP) shows that celecoxib has no significant affinity (K_i > 10 μM) for brain biogenic amines, receptors or transporters. To derive conditions of radiolabeling for obtaining optimum yield in minimum time, experiments were first performed under non-radioactive conditions. After reacting precursor **5** with KF-Kryptofix® at elevated temperature, in solvents such as acetonitrile or dimethylsulfoxide, only negligible amount (<3%) of celecoxib **6** was formed after deprotecting the sulfonamide group (1:1; TFA/DCM). Whereas, heating **5** with tetrabutylammonium fluoride at 135 °C (TBAF) in DMSO for 40 min followed by sulfonamide deprotection afforded **6** in good yield (80%, Scheme 1).

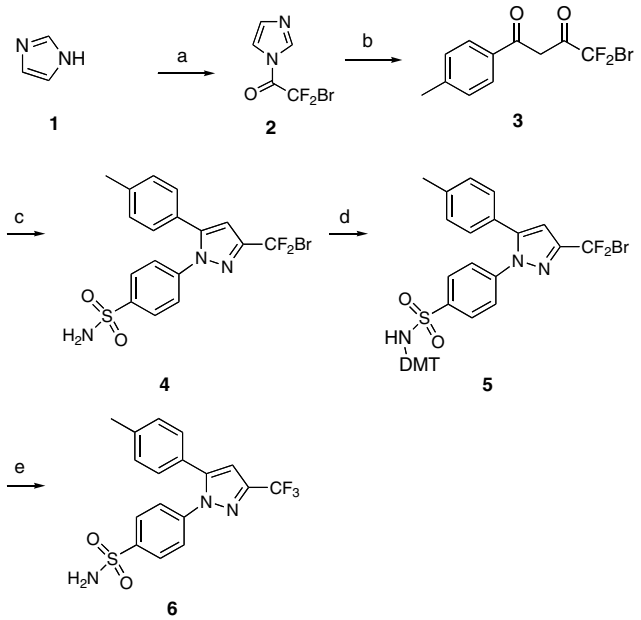

Scheme 1. Synthesis of celecoxib and radiolabeling precursor. Reagents and conditions: (a) 2-bromo-2,2-difluoroacetyl chloride, rt, THF, 90%; (b) *p*-tolylethanone, THF, reflux, 65%; (c) 4-hydrazinobenzenesulfonamide, ethanol, reflux, 45%; (d) DMT/Cl, TEA, CH_2Cl_2, 82%; (e) 1—TBAF (4 equiv), DMSO, 135 °C, 40 min; 2—TFA/DCM (1:1), 60 °C, 5 min, 80%.

2.2. Radiochemistry

Incorporation of [^{18}F]fluorine to precursor **5** was also not effective using [^{18}F]KF-Kryptofix® as the radiolabeling reagent, even under rigorous conditions such as using high temperature and microwave irradiation. Optimum yield of [^{18}F]**6** was obtained while heating precursor **5** with [^{18}F]TBAF[22] in DMSO for 20 min at 135 °C followed by treating with a 1:1 mixture of TFA and DCM (Scheme 2). The reaction mixture was purified by RP-HPLC followed by passing through a C-18 Sep-Pak® cartridge. The radiochemical yield of [^{18}F]**6** was 10 ± 2% (n = 6) at the end of synthesis (EOS). The chemical identity of [^{18}F]**6** was confirmed by co-injecting the radio-product with non-radioactive celecoxib on an analytical RP-HPLC. The chemical and radiochemical purities of [^{18}F]**6** were found to be >99% with a specific activity of 120 ± 40 mCi/μmol at EOB. Multiple mobile phases were used to determine the purities of the radioligand. Our efforts to improve the yield and specific activity of [^{18}F]**6** were not effective. We observed that lowering the temperature or decreasing the time of experiment did not improve the outcome of the reaction. We hypothesize that in the reaction mixture, a competitive [^{19}F]$^-$ to [^{18}F]$^-$ exchange may compete with [^{18}F]$^-$ incorporation, resulting in low yield and specific activity of [^{18}F]celecoxib.[23]

2.3. In vitro stability

In vitro stability of [^{18}F]celecoxib was determined in ethanol and 10% ethanol–saline using silica gel TLC, in which [^{18}F]fluoride stays at the origin and [^{18}F]celecoxib stays at the solvent front.[18] No significant

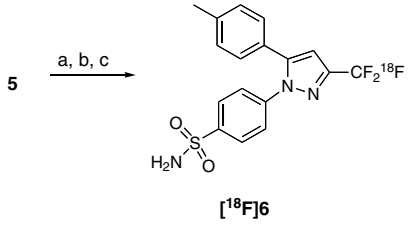

Scheme 2. Radiosynthesis of [^{18}F]celecoxib. Reagents and conditions: (a) 1—[^{18}F]TBAF, DMSO, 135 °C, 20 min; (b) TFA/DCM (1:1), 60 °C, 5 min; (c) Semipreparative HPLC purification.

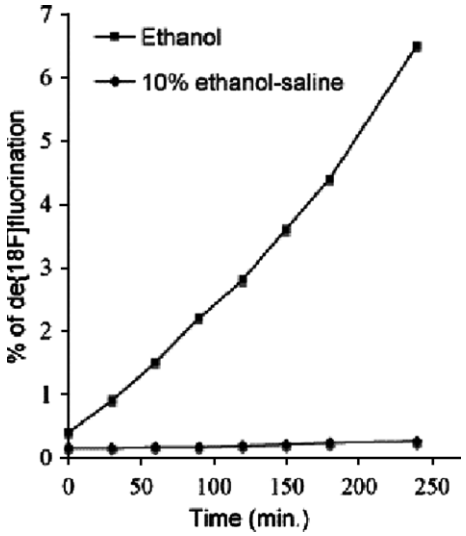

Figure 1. In vitro stability of [^{18}F]celecoxib. Data points presented are the average determinations from representative experiments repeated at least on two-independent occasions with similar results.

de[^{18}F]fluorination was observed for [^{18}F]celecoxib formulation in ethanol up to 4 h, but a low rate of de[^{18}F]fluorination (6.5% in 4 h) was observed for the radiotracer formulation in saline containing 10% ethanol (Fig. 1).

2.4. In vivo imaging in rats

Since the in vitro de[^{18}F]fluorination rate of [^{18}F]celecoxib was relatively slow in the imaging time-frame (2–3% in 90–120 min), in vivo imaging was performed in rats using a small animal PET Scanner (microPET). PET images in a rat during 0–20 min (A) and 60–120 min (B) are shown in Figure 2. The PET images show significant bone uptake, most likely be attributed to in vivo de[^{18}F]fluorination of [^{18}F]**6** (Fig. 2B). The time–activity curves (TACs) generated from the PET studies show higher skeleton uptake of [^{18}F]**6** compared to brain or heart, regions where COX-2 is known to be present (Fig. 3).[24] The uptake ratio of [^{18}F]**6** in heart, cerebellum, and rest of the brain with reference to skeleton at 112 min was found to be 0.70, 0.54 and 0.45, respectively (Fig. 3).

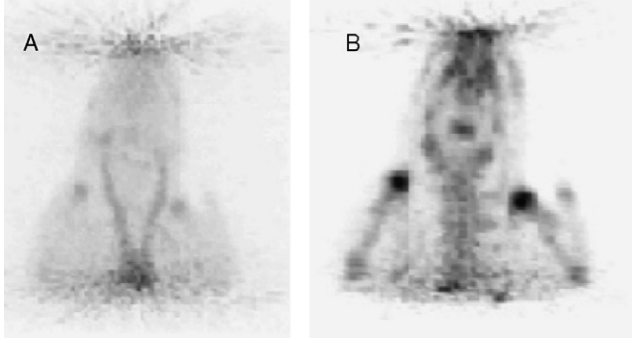

Figure 2. microPET images of [^{18}F]celecoxib in rat. PET images of [^{18}F]celecoxib in rat (images are normalized to the injected dose). (A) Sum of 0–20 min PET images; (B) sum of 60–120 min PET images.

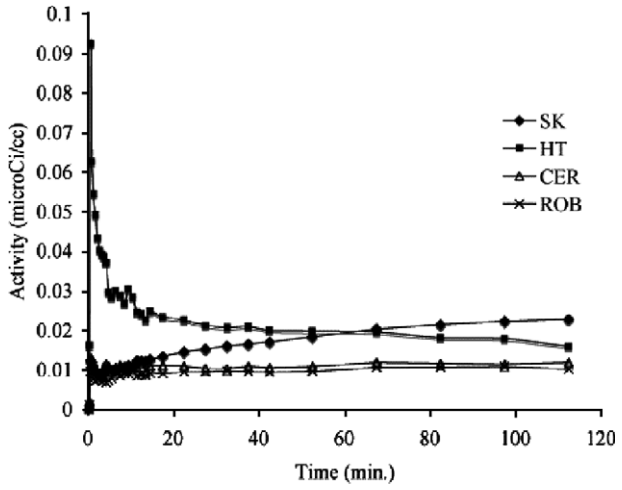

Figure 3. Time–activity curves of the radioactivity in rat after the injection of [^{18}F]celecoxib (CER, cerebellum; HT, heart; SK, skeleton; ROB, rest of brain).

2.5. PET studies in baboon

PET studies in anesthetized baboon show that [^{18}F]celecoxib (dose = 2.0 ± 0.4 mCi, specific activity = 120 ± 40 mCi/μmol) penetrated the BBB and accumulated in brain (Fig. 4).[25] The TACs of several brain regions and skull were examined and show relatively poor skull uptake indicating a low degree of in vivo de[^{18}F]fluorination of radioligand (Fig. 5) in baboon. Uptake of [^{18}F]**6** peaked in most regions within 3.5–13 min and then declined relatively slowly. The fastest washout was observed in skull followed by cerebellum, hippocampus, cingulate cortex, putamen, caudate, and thalamus. The distribution of [^{18}F]**6** accumulation in baboon brain is consistent with known distribution of COX-2.[26–29] The binding ratios of thalamus, caudate, putamen, cingulate, hippocampus, and cerebellum in comparison to skull are 1.60, 1.48, 1.46, 1.43, 1.41, and 1.20, respectively, at 115 min. The brain to skull ratio of baboon is 3–4 times higher than the ratio obtained for rats indicating a lower rate of de[^{18}F]fluorination in non-human primates in comparison to rodents. The metabolite analyses show that [^{18}F]celecoxib undergoes fast metabolism.[25] Polar metabolites were found in baboon plasma and the % of unmetabolized fractions at 2, 4, 12, 30, and 60 min are 93.2%, 84.9%, 47.5%, 30.2%, and 17.0%, respectively (Fig. 6).[24]

3. Conclusion

Synthesis of [^{18}F]celecoxib was achieved via a bromide to [^{18}F]fluoride displacement reaction in 10 ± 2% yield (EOS) and a specific activity of 120 ± 40 mCi/ μmol. Poor specific activity of [^{18}F]celecoxib obtained from the bromine to [^{18}F]fluorine displacement reaction may be attributed to the competitive defluorination from **5**, which may dilute the [^{18}F]anion during the labeling

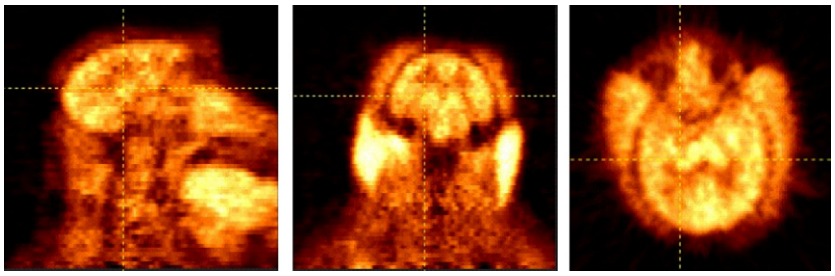

Figure 4. Sum of the (0–120 min) PET images of baboon brain after the injection of 1.2 mCi [^{18}F]celecoxib. First column, sagittal; middle column, coronal; last column, axial views.

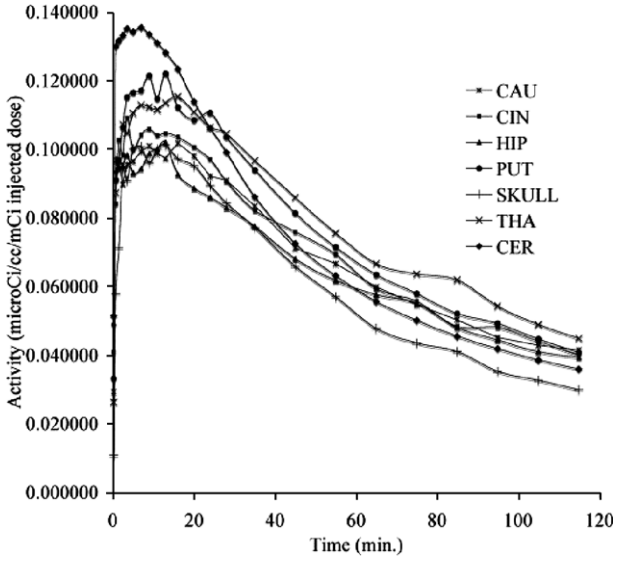

Figure 5. Time–activity curves of the radioactivity in baboon after the injection of [^{18}F]celecoxib (CIN, cingulate; CER, cerebellum; CAU, caudate; HIP, hippocampus; PUT, putamen; THA, thalamus).

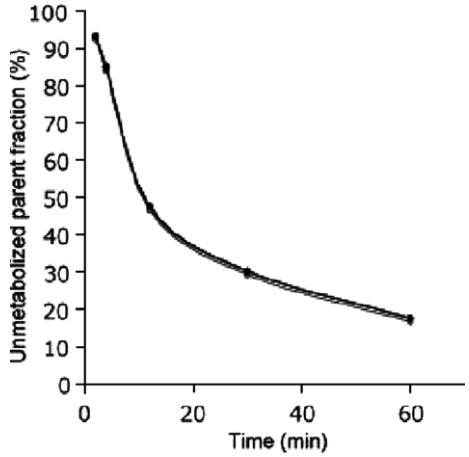

Figure 6. Unmetabolized parent fraction of [^{18}F]celecoxib in baboon plasma. Filled circles represent the average of two studies.

process. The radiotracer was found to be stable in ethanol solution, but de[^{18}F]fluorinated slowly in 10% ethanol–saline solution. microPET studies in rat show that [^{18}F]celecoxib has uptake in heart and brain. Due to the in vivo de[^{18}F]fluorination of [^{18}F]celecoxib in normal rats the ligand is unlikely to allow imaging of COX-2 expression in rats. However, the de[^{18}F]fluorination rate is lower in baboon and could be much slower in human subjects due to a slower metabolism. Further studies are required to demonstrate the utility of [^{18}F]celecoxib in human subjects as a PET tracer for the in vivo imaging of COX-2 expression, and specifically an improved radiolabeling method is needed for routine human use.

4. Experimental

4.1. General

The commercial chemicals used in the synthesis were purchased from Sigma–Aldrich Chemical Co. or Fisher Scientific Inc. and were used without further purification. Melting points were determined on a Fisher melting point apparatus and are uncorrected. ^{1}H NMR spectra were recorded on a Bruker PPX 300 and 400 MHz spectrometer. ^{19}F NMR spectra were generated on Bruker PPX 282.5 MHz spectrometer. Spectra are obtained in $CDCl_3$ and chemical shifts are reported in ppm relative to TMS for ^{1}H and $CFCl_3$ for ^{19}F as internal standards. The mass spectra were recorded on JKS-HX 11UHF/HX110 HF Tandem Mass Spectrometer in the FAB+ and EI+ mode. Semipreparative HPLC analyses were performed using a Waters 1525 HPLC system. Semipreparative analyses were performed by Phenomenex, Prodigy ODS(3) 10×250 mm, 10 μ column and analytical studies were performed by Phenomenex, Prodigy ODS(3) 4.6×250 mm, 5 μ column ($\lambda = 254$ nm). Flash column chromatography was performed on silica gel (Fisher 200–400 mesh) using the solvent system indicated in the experimental procedure for each compound. [^{18}F]Fluoride was generated from RDS112 cyclotron (Siemens, Knoxville,). The radio-TLC was performed on silica gel plates (EM science, silica gel 60 F_{254}) using Bioscan, AR-2000 Instrument and ethanol as the mobile phase. microPET studies were performed with Seimens R4, Microsystem Inc.

4.2. Chemistry

4.2.1. 4-Bromo-4,4-difluoro-1-*p*-tolylbutane-1,3-dione (3). At 0 °C, bromodifluoroacetyl chloride (386 mg, 2 mmol) was added to a solution of imidazole (285 mg, 4.2 mmol) in 2.5 mL anhydrous THF. The

solution was warmed to room temperature and stirred for an additional hour. The precipitate formed was filtered off and the filtrate was washed with ether (2× 5 mL), the combined filtrates were evaporated and dried under high vacuum to give compound **2** (400 mg, 90%). The imidazole derivative **2** thus obtained was dissolved in anhydrous THF (1 mL) and added to a previously stirred solution of 4′-methyl acetophenone (268 mg, 2 mmol) in 10 mL THF treated with NaHMDS solution (1 M in THF, 3 mL, 3 mmol) at −78 °C. After the addition of **2**, the reaction mixture was warmed to room temperature and stirred for 1 h. The reaction was quenched by adding saturated ammonium chloride solution and diluted with water (10 mL). The products were extracted into ethyl acetate (3× 25 mL), washed with water and brine, and dried over anhydrous magnesium sulfate. Solvent was evaporated under reduced pressure and the product was purified using silica gel column chromatography using 15% ethyl acetate in hexane to afford dione **3** (380 mg, 65%) as a viscous liquid.

Compound **3**: ^{1}H NMR (300 MHz, $CDCl_3$) δ: 7.83 (d, $J = 9$, 2H), 7.26 (d, $J = 9$, 2H), 6.55 (s, 1H), 2.43 (s, 3H); HRMS (EI^+) calculated for $C_{11}H_{10}O_2BrF_2$: 289.9754. Found: 289.9759.

4.2.2. 4-[3-(Bromodifluoromethyl)-5-*p*-tolylpyrazol-1-yl]-benzenesulfonamide (4). 1,3-Dione (**3**, 291 mg, 1 mmol) and 4-hydrazino-sulfonamide (224 mg, 1 mmol) were dissolved in anhydrous ethanol (20 mL) and the mixture was refluxed for 16 h. Ethanol was evaporated, and the residue was dissolved in ethyl acetate, washed with water and brine. The organic layer was dried over anhydrous $MgSO_4$, concentrated, and the product was purified by silica gel column chromatography using 20% ethyl acetate in hexane to afford sulfonamide **4** as a white solid (200 mg, 45%), mp 184–185 °C.

Compound **4**: ^{1}H NMR (300 MHz, $CDCl_3$) δ: 7.95 (d, $J = 9$, 2H), 7.51 (d, $J = 9$, 2H), 7.15 (m, 4H), 6.76 (s, 1H), 4.98 (s, 2H), 2.39 (s, 3H); ^{19}F NMR (282.5 MHz, $CDCl_3$) δ: −42.31 (s); HRMS (EI^+) calculated for $C_{17}H_{15}O_2N_3BrF_2S$: 443.0017. Found; 443.0064.

4.2.3. *N*-[Bis(4-methoxyphenyl)phenylmethyl]-4-[3-(bromo-difluoromethyl)-5-*p*-tolylpyrazol-1-yl] benzenesulfonamide (5). To a solution of sulfonamide **4** (256 mg, 0.6 mmol) in dichloromethane (10 mL) at 0 °C was added dimethoxytrityl chloride (245 mg, 0.72 mmol) in dichloromethane (5 mL). Triethylamine (0.2 mL, 1.45 mmol) was added to the above solution and stirred at room temperature for 1 h after which the solution was evaporated under reduced pressure and the residue was directly charged onto a silica gel column. The product was eluted using 15% ethyl acetate in hexane (350 mg, 82%) as a colorless solid; mp 135–136 °C.

Compound **5**: ^{1}H NMR (400 MHz, $CDCl_3$) δ: 7.20–7.12 (m, 17H), 6.71 (m, 4H), 5.79 (s, 1H), 3.75 (s, 6H), 2.35 (s, 3H); ^{19}F NMR (282.5 MHz, $CDCl_3$) δ: −42.10 (s); HRMS (FAB^+) calculated for $C_{38}H_{32}O_4N_3BrF_2S$: 744.1343. Found; 744.1343. Elemental analysis calculated for $C_{38}H_{32}O_4N_3BrF_2S$, C, 61.29; H, 4.33; N, 5.10. Found: C, 61.41; H, 4.62; N, 5.38.

4.2.4. Synthesis of celecoxib (6) from bromoderivative 5. Compound **5** (51 mg, 0.07 mmol) was dissolved in DMSO (2 mL) and 0.27 mL (0.27 mmol) TBAF in THF was added to it. The solution was heated at 135 °C for 40 min after which it was cooled to room temperature and 5 mL of 20% TFA in DCM was added. The solution was stirred for 5 min and treated with water (2 mL). The product was extracted into ethyl acetate (3× 5 mL), washed with water and brine, and purified by silica gel column chromatography using 40% ethyl acetate in hexane to afford celecoxib (**6**) (21 mg, 80% yield). ^{1}H and ^{19}F NMR of synthesized **6** are identical to the reported data.[4]

4.3. Radiosynthesis of [^{18}F]celecoxib

The aqueous solution of [^{18}F]fluoride generated from RDS 112 cyclotron is passed through an activated QMA and eluted with a mixture of 50 μmol of tetrabutylammonium bicarbonate in 1 mL of acetonitrile to a reaction vial. The reaction mixture was heated at 110 °C under a stream of argon while it dried azeotropically with the addition of acetonitrile (3× 0.4 mL). A solution of 3 ± 0.5 mg of precursor **5** in 0.5 mL of anahydrous DMSO was added to the reaction vial, sealed, mixed well, and heated for 20 min. The reaction mixture was allowed to cool at room temperature and 1 mL of 50% TFA in DCM was slowly added. The solution was purged with argon at 60 °C for 5 min to remove DCM. The reaction mixture was then treated with 0.5 mL of 1:1 methanol/water, mixed well and further diluted with 4 mL water. The reaction mixture was subsequently passed through a classic C-18 Sep-Pak cartridge, washed with 20 mL water to remove unreacted [^{18}F]fluoride and other polar impurities, eluted with 1 mL of acetonitrile, and injected onto a semipreparative RP-HPLC (mobile phase; 60:39:1, acetonitrile/water/acetic acid, flow rate 5 mL/min). The product fraction with a retention time (t_R) of 11 min based on γ-detector was collected, diluted with 100 mL of deionized water, and passed through a classic C-18 Sep-Pak® cartridge. The DMT-deprotected precursor appears at 12–14 min. Reconstitution of the product in 1 mL of absolute ethanol afforded [^{18}F]celecoxib. A portion of the ethanol solution was analyzed by analytical HPLC (mobile phase; 60:39:1, acetonitrile/water/acetic acid, flow rate 1 mL/min, $t_R = 10$ min) to determine the specific activity, chemical and radiochemical purities. The chemical and radiochemical purities of [^{18}F]celecoxib were confirmed by RP-HPLC (mobile phase; 1:1 acetonitrile/50 mM sodium phosphate, flow rate: 2 mL/min, $t_R = 14$ min).

4.4. PET studies of [^{18}F]celecoxib in rodent

All animal experiments were carried out with the approval of the Institutional Animal Care and Use Committees of Columbia University Medical Center and the New York State Psychiatric Institute. Sprague–Dawley rats (male) weighing 300–400 g (Hilltop

Lab Animals, NY) were anesthetized with isoflurane (1–5%) and positioned head and upper thorax at the center of the field of view of a microPET R4 camera (Seimen's Microsystems, Inc., Model R4). A polyethylene catheter (PE90, 1.27 mm od, Intramedic) filled with heparinized saline was inserted into the left femoral vein for radioligand injection and a terminal KCl (4 M) injection at the conclusion of the experiment. The femoral arteries were cannulated (PE50, 0.965 mm od, Intramedic) for measurement of arterial pressure, blood gases, and hematocrit. A tracheotomy was performed (PE360, Intramedic) for artificial ventilation. Transmission scans were acquired with a rotating germanium-68 point source and used attenuation correction. [^{18}F]**6** (0.2 mCi) was injected into the left femoral vein and initiated camera acquisition. List-mode data were collected for 120 min and reconstructed using attenuation correction and Fourier rebinning. The dynamic images were reconstructed using a filtered back-projection algorithm and interpolated to give nCi/cc (microPET Manager, Concorde Microsystems Inc.). The regions of interest (ROIs) were drawn on the PET images. Time–activity curves were generated for ROIs including heart, bone, and brain.[30,31]

Acknowledgments

Pfizer Inc. provided funding for this investigator initiated grant request. The authors thank the NIMH-PDSP for the pharmacologic screen of celecoxib. Ms. Anna R. Cooper provided technical assistance for the microPET studies.

References and notes

1. Lipsky, P. E. *Am. J. Med.* **1999**, *106*, 15473–15480.
2. Masferrer, J. L. *Proc. Natl. Acad. Sci. U.S.A.* **1994**, *91*, 3228–3232.
3. Talley, J. J. *Prog. Med. Chem.* **1999**, *36*, 201–234.
4. Penning, T. D.; Talley, J. J.; Bertenshaw, S. R.; Carter, J. S.; Collins, P. W.; Docter, S.; Graneto, M. J.; Lee, L. F.; Malecha, J. W.; Miyashiro, J. M.; Rogers, R. S.; Rogier, D. J.; Yu, S. S.; Anderson, G. D.; Burton, E. G.; Cogburn, J. N.; Gregory, S. A.; Koboldt, C. M.; Perkins, W. E.; Seibert, K.; Veenhuizen, A. W.; Zhang, Y. Y.; Isakson, P. C. *J. Med. Chem.* **1997**, *40*, 1347–1365.
5. Chan, C.-C.; Boyce, S.; Brideau, C.; Charleson, S.; Cromlish, W.; Ethier, D.; Evans, J.; Ford-Hutchinson, A. W.; Forrest, M. J.; Gauthier, J. Y.; Gordon, R.; Gresser, M.; Guay, J.; Kargman, S.; Kennedy, B.; Leblanc, Y.; Leger, S.; Mancini, J.; O'Neill, G. P.; Ouellet, M.; Patrick, D.; Percival, M. D.; Perrier, H.; Prasit, P.; Rodger, I.; Tagari, P.; Therien, M.; Vickers, P.; Visco, D.; Wang, Z.; Webb, J.; Wong, E.; Xu, L.-J.; Young, R. N.; Zamboni, R.; Riendeau, D. *J. Pharm. Exp. Ther.* **1999**, *290*, 551–560.
6. Talley, J. J.; Brown, D. L.; Carter, J. S.; Graneto, M. J.; Koboldt, C. M.; Masferrer, J. L.; Perkins, W. E.; Rogers, R. S.; Shaffer, A. F.; Zhang, Y. Y.; Zweifel, B. S.; Seibert, K. *J. Med. Chem.* **2000**, *43*, 775–777.
7. Fitz, G. A. *Nat. Rev. Drug Disc.* **2003**, *2*, 879–890.
8. Gately, S. T. *Prog. Drug Res.* **2005**, *63*, 207–225.
9. Giovannini, M. G.; Scali, C.; Prosperi, C.; Bellucci, A.; Pepeu, G.; Casamenti, F. *Int. J. Immunopathol. Pharmacol.* **2003**, *16*, 31–40.
10. Massoud, T. F.; Gambhir, S. S. *Genes Dev.* **2003**, *17*, 545–580.
11. Phelps, M. E. *Proc. Natl. Acad. Sci. U.S.A.* **2000**, *97*, 9226–9233.
12. Isakson, P. C.; Clarkson, V.; Seibert, K.; Talley, J. J. *PCT Int. Appl.* **2000**, 6045773.
13. McCarthy, T. J.; Sheriff, A. U.; Graneto, M. J.; Talley, J. J.; Welch, M. J. *J. Nucl. Med.* **2002**, *43*, 117–124.
14. de Vries, E. F. J.; van Waarde, A.; Buursma, A. R.; Vaalburg, W. *J. Nucl. Med.* **2003**, *44*, 1700–1706.
15. Toyokuni, T; Satyamurthy, N; Herschman, H. R; Phelps, M. E; Barrio, J. R. *PCT Int. Appl.* WO 2003089013, 2003, 60 pp.
16. Mann, J. J.; Kumar, J. S. D. WO 2005120584, 2005, 51 pp.
17. Majo, V. J.; Prabhakaran, J.; Simpson, N. R.; Van Heertum, R. L.; Mann, J. J.; Kumar, J. S. D. *Bioorg. Med. Chem. Lett.* **2005**, *15*, 4268–4271.
18. Toyokuni, T.; Kumar, J. S. D.; Walsh, J. C.; Shapiro, A.; Talley, J. J.; Phelps, M. E.; Herschman, H. R.; Barrio, J. R.; Satyamurthy, N. *Bioorg. Med. Chem. Lett.* **2005**, *15*, 4699–4702.
19. Prabhakaran, J.; Majo, V. J.; Simpson, N. R.; Van Heertum, R. L.; Mann, J. J.; Kumar, J. S. D. *J. Labelled Compd. Radiopham.* **2005**, *48*, 887–895.
20. Yuji, K.; Yumiko, K.; Sayaka, S.; Takashi, T.; Hiroyuki, K.; Yasushi, K.; Chiaki, Y.; Kazuo, M.; Koh-ichi, S.; Nagara, T.; Kazue, O.; Hideo, S. *Nucl. Med. Biol.* **2006**, *33*, 21–27.
21. Staab, H. A.; Walther, G. *Ber.* **1962**, *95*, 2070–2072.
22. Alauddin, M. M.; Conti, P. S.; Mathew, T.; Fissekis, J. D.; Surya Prakash, G. K.; Watanabe, K. A. *J. Fluorine Chem.* **2000**, *106*, 87–91.
23. Das, M. K.; Mukherjee, Y. *Appl. Radiat. Isot.* **1993**, *44*, 835–842.
24. Yasojima, K.; Schwab, C.; McGeer, E. G.; McGeer, P. L. *Brain Res.* **1999**, *830*, 226–236.
25. Kumar, J. S. D.; Majo, V. J.; Sullivan, G. M.; Prabhakaran, J.; Van Heertum, R. L.; Parsey, R. V.; Mann, J. J. *Bioorg. Med. Chem.* **2006**, *14*, 4029–4034.
26. Kaufmann, W. E.; Worley, P. F.; Peggi, J.; Bremer, M.; Peter Isakson, P. *Proc. Nat. Acad. Sci. U.S.A.* **1996**, *93*, 2317–2321.
27. Minghetti, L. *J. Neuropathol. Exp. Neurol.* **2004**, *63*, 901–910.
28. Breder, C. D.; Dewitt, D.; Kraig, R. P. *J. Comp. Neurol.* **1995**, *355*, 296–315.
29. Ho, L.; Pieroni, C.; Winger, D.; Purohit, D. P.; Aisen, P. S.; Pasinetti, G. *J. Neurosci. Res.* **1999**, *57*, 295–303.
30. Watson, C. C.; Newport, D.; Casey, M. E. *Aix-les-bains*, France, **1995**, pp 215–219.
31. Woods, R. P.; Cherry, S. R.; Mazziotta, J. C. *J. Comput. Assist. Tomogr.* **1992**, *16*, 620–633.